Locally Produced UHPC: The Influence of Type and Content of Steel Fibres

Ingrid Lande
M.Sc, PhD Research Fellow
Department of Engineering sciences
Faculty of Engineering and Science
University of Agder
Jon Lilletuns vei 9, 4879 Grimstad
e-mail: ingrid.lande@uia.no

Rein Terje Thorstensen
Professor
Department of Engineering sciences
Faculty of Engineering and Science
University of Agder
Jon Lilletuns vei 9, 4879 Grimstad
e-mail: rein.t.thorstensen@uia.no

ABSTRACT
Ultra-high performance concrete might be a competitive alternative to normal concrete for some purposes. But despite research efforts during decades, utilisation is still not widespread. Reasons include limited competence and material availability. This paper presents one step of a research initiative aimed at facilitating the use of UHPC in Norway. The step presented here comprises the accumulated results from investigations on the influence steel fibres (content, type, and hybrid combination) have on material strength and deformation behaviour of locally produced UHPC, made with constituents found in southern Norway. 231 specimens were tested, spanning nine UHPC mixes. Digital Image Correlation (DIC) was successfully used to study crack propagation. Compressive strength of 166 MPa and E-modulus of 46 GPa were obtained, not being influenced by fibre content. The flexural tensile strength was found to be strongly dependent on variations in

steel fibre properties and mix design. The highest flexural tensile strength was obtained for prisms with micro straight steel fibres alone, or in 50% combination with macro hooked-end fibres. The experimental results are considered in a theory-informed discussion. Suggestions are made on the use of steel fibres in locally produced UHPC, potentially lowering the cost by 30%.

Keywords: Ultra-High Performance Concrete (UHPC), Local materials, Material properties, Steel fibres, Digital Image Correlation (DIC)

1.   INTRODUCTION

Though the term Ultra-High Performance Concrete (UHPC) has been used for decades, a unified definition of required material properties to merit this notation has not yet been accepted. In a novel paper by five leading researchers within the field, the following suggestion is made for defining UHPC class materials [1]: "*(1) a compressive strength greater than 120 MPa; (2) a disconnected pore structure that significantly reduces permeability and thus enhances durability; and (3) sufficient fiber reinforcement to allow for sustained postcracking tensile resistance that exceeds a minimum cracking strength of 5 MPa*". Research work over at least 50 years [2] has been manifested through various applications worldwide both within the bridge sector and the construction industry in general. Some countries (e.g., Switzerland, France, Germany, South Korea, Malaysia, Canada, and the US) have successfully implemented UHPC in different bridge projects as field-cast connections between prefabricated concrete bridge elements, on-site rehabilitation overlays or as the primary material in new road or pedestrian bridges [1]. In most of these countries, the implementation has been motivated through government agencies [3]. The US Federal Highway Administration (FHWA) has been at the forefront of both the research work and pilot applications. A series of reports by FHWA, e.g. a state-of-the-art report [4], has created a foundation for the implementation of UHPC in the bridge sector.

Proprietary UHPC materials are utilised in the majority of the existing UHPC structures. These commercially available products are offered from a limited number of producers worldwide, leading to an oligopolistic market situation with high costs compared to expectations in a competitive market. The price of the proprietary UHPC products is found to be 20 times higher than conventional concrete materials [5, 6]. The actual production cost of UHPC using local materials in the US is about half of this [6]. Most of the cost is attributed to the extensive use of micro straight steel fibres. The high cost and low local availability are two aspects that have limited wider use of UHPC. Smart use of UHPC is frequently claimed to have the potential for reducing CO_2 emission [7] and the life cycle cost of concrete structures. A reduction in material cost might be an important driving force towards more widespread implementation. The potential for producing high-quality UHPC with local materials has been proven over and over by a variety of researchers, e.g., [8-12]. Scandinavian experiences have been reported since the 1980s (e.g. [13]), also regarding an industrial mock-up test [14] and commercial applications (e.g., [15, 16]). In a not yet scientifically reported industrial-academic cooperation ("New applications of UHPC", financially supported by the Research Council of Norway), high-quality UHPC was successfully produced from local constituents in the full-scale production facilities of an ordinary concrete supplier in Norway. Subsequently, UHPC with corresponding properties was reproduced in laboratory scale, utilising local constituents from other sources and through only minor adjustments in the mix proportioning [17]. However, Scandinavian participation in the development towards widespread utilisation of UHPC seems scarce.

High contents of high strength straight micro steel fibres (often 13 mm in length and 0.2 mm in diameter) is the main cost contributor in UHPC, responsible for half of the price [6]. It is also one of the main attributes of high CO_2 emissions. Large parts of these emissions stem from the process of wet wire drawing of the fibres into small diameters (around 0.2 mm) [18]. To reduce this impact, Stengel and Schießl [18] recommended using fibres with larger diameters. Several studies (e.g., [19-24]) have focused on more efficient use of steel fibres in UHPC through utilising various fibre types. Some have focused on increasing the pull-out strength by either increasing the fibre length or by using deformed fibres (e.g., [19, 20, 23]). Another concept is utilising hybrid fibre configuration (e.g., in [21, 22, 24]). The principle is to combine different fibres, often micro straight fibres and macro deformed fibres, utilising the synergy of their individual properties [25]. Prior research on hybrid fibre reinforcement used macro fibres with length up to 30 mm [26], while limited investigations have focused on the effects of larger macro hooked-end fibres with fibre length above 50 mm. These are frequently used in normal fibre reinforced concrete and are easily available at a low cost. It would be beneficial for local production of UHPC if these fibres could at least partially substitute micro fibres, while retaining UHPC properties. Utilising fibres made for normal concrete in a high strength UHPC matrix introduces a risk of fibre rupture, due to the lower tensile strength of the fibres (around 1000 MPa) combined with the high mechanical anchorage at the fibre ends.

This paper presents one step of a research initiative on understanding the material properties and behaviour of UHPC made from local materials, with the long-term goal of facilitating the use of UHPC in Norway. The work presented in this paper was focused on experimental investigations on UHPC made from local constituents found in southern Norway. The aim was twofold:
- Developing high-quality non-proprietary UHPC mixes using locally available materials.
- Investigating the influence of steel fibres (content, type, and combination) on material properties and deformation behaviour of local UHPC mixes.

The key material properties investigated in this study was compressive strength, modulus of elasticity (E-modulus) and flexural tensile strength and behaviour. A Digital Image Correlation system (DIC) was used to monitor and analyse the deformation behaviour of prisms in flexure. The experiments included variations in mix composition, fibre configuration, test specimen geometry and curing regime, comprising 231 tested specimens.

2.   LITTERATURE REVIEW OF COMPOSITION AND PROPERTIES

UHPC has developed through several stages, spanning from laboratory materials utilising high pressure (autoclaving) and elevated temperatures (250 to 400°C) to create extremely high compressive strength (above 490 MPa) and flexural tensile strength (above 45 MPa) [27], to a material suitable for structural applications, producible from locally available constituents and by using traditional production equipment. In the following, a brief literature review is given of existing data on constituents, mix design and relevant properties identified through the research papers on both proprietary brands and locally produced UHPC materials.

2.1   UHPC constituents and mix design

The constituents used in UHPC is similar to those used in conventional concrete, such as aggregates, cement, microsilica, superplasticiser (SP) and water. However, the paste phase (cement, microsilica, fillers, water, SP) usually stands for about 2/3 of the volume in UHPC

materials, while the particle phase is only 1/3 and consists of fine particles only with maximum grain size (D_{max}) often lower than 1 mm [2]. In the state-of-the-art report by FHWA [4], recommendations on D_{max} are 0.8 mm. The paste phase consists of large contents of cement and microsilica. Normally 700 to 1100 kg per cubic meter of cement is applied with a microsilica ratio of around 0.25 to the mass of cement. In some mixes, other types of cementitious binders (e.g., fly ash, ground granulated blast-furnace slag or limestone powder) are used in addition or to reduce the cement or microsilica content [22, 28]. Usually, water/binder-ratio (w/b-ratio) around 0.2 is applied, made possible through a high content of SP. In contrary to conventional concrete, fibres are a necessary component in UHPC to reduce brittleness in compression and tension and give exploitable tensile strength. In proprietary UHPC products, straight micro steel fibres with a length (l_f) around 10-20 mm and diameter (d_f) of 0.2-0.4 mm is applied with fibre content between 2 and 6 vol.% [12]. Recommendations on mix proportions of UHPC class materials can be found e.g. in [6, 29] and reads as follows:

- Microsilica content and other cementitious binders both 25% of the mass of cement.
- Aggregate to cement ratio between 1 and 2.
- Water/cement (w/c-ratio) between 0.2 and 0.3.
- Fibre content between 1 and 2 vol.%.

Mix proportions of both proprietary UHPC products and UHPC mixes found in research, are summarised in Table 1.

Table 1 – Mix composition of proprietary UHPC products and UHPC mixes in research.

	Proprietary UHPC [a]	Yoo et al.	Meng & Khayat	Yu et al.	Le Hoang & Fehling	Gesoglu et al.
Materials	kg/m³	kg/m³	kg/m³	kg/m³	kg/m³	kg/m³
Cement	712-1114	789	641-675	582-896	772-795	960
Microsilica	169-275	197	41-43	24 [b]	164-169	240
Other binders	N/A	N/A	367-422	0-275	N/A	N/A
Fine sand	730-1325	1104	943-992	1256-1337	1134-1169	706-794
SP	31-40	53	23-113	43-46	23-24	45-57
Water	109-211	160	228	153-179	182-188	234
Steel fibres	156-470	39-156	0-390	N/A	0-236	0-157
w/b	0.14-0.16 [c]	0.2	0.2	0.165-0.2	0.21	0.195
D_{max} [mm]	0.5-6	0.3	4.8	2	0.5	2.5
Reference	[3, 4, 12]	[21, 30]	[22]	[28]	[31]	[20]

[a] Ductal®, CEMTEC multiscale®, BSI®, CRC®. [b] Nano-silica. [c] Calculated from given w/c-ratio. N/A - Not available.

High particle packing density is important to obtain the special material properties of UHPC. Different approaches have been applied [32]. One method used in several studies (e.g. in [12, 28, 29]), is the modified version [33] of the Andreasen and Andersen model for granular materials [34]. The particle distribution curve reads as follows (Eq. 1):

$$\text{CPFT} = \left(\frac{D - D_{min}}{D_{max} - D_{min}}\right)^q \tag{1}$$

where CPFT is the cumulative per cent finer than size D, D is the varying particle size, D_{min} and D_{max} represent the smallest and largest particle size of the distribution, respectively. The q-value represents the distribution coefficient and determine the curvature of the cumulative PSD. The curve acts as a target for the densest possible particle composition.

2.2   UHPC strength properties

Table 2 lists some material properties of UHPC found in the literature. Compressive strength exceeding 120 MPa is found in the research literature as well as for proprietary UHPC. E-modulus values are ranging from 39 to 70 GPa.

Table 2 – Material properties of proprietary UHPC product and UHPC mixes in research.

Material properties	Proprietary UHPC [a]	Yoo et al.	Meng & Khayat	Yu et al.	Le Hoang & Fehling	Gesoglu et al.	SOA by FHWA
Compressive strength [MPa]	180-225	185-220	140-166	100-117[b]	199-219	137-162[b]	140-200
E-modulus [GPa]	55-59	N/A	N/A	N/A	52-55	39-45[b]	40-70
Flexural tensile strength [MPa]	40-50	34-49	10-27	12-19[b]	N/A	7-14[b,c]	N/A
Density [kg/m³]	2440-2550	N/A	N/A	N/A	N/A	N/A	N/A
Reference	[35]	[21, 30]	[22]	[28]	[31]	[20]	[4]

SOA – State-of-the-art report. [a] Ductal®. [b] Read-off from figures. [c] Notched prism. N/A – Not applicable.

The inclusion of discrete steel fibres has shown to give high tensile properties, often characterised by a multiple cracking phase after first cracking. At high dosages, it also creates deflection-hardening behaviour. Table 2 shows that flexural strength up to 50 MPa is achieved under three- or four-point bending tests. These flexural tests are often used to characterise the tensile capacity properties, probably due to the easiness of execution. Sometimes also direct tensile strength tests are performed, often showing tensile cracking strength values from 6 to 10 MPa [4].

An increase in material properties can be achieved through curing at elevated temperatures, usually at 90°C for 48 hours (95% relative humidity and without high pressure). Studies have shown improved compressive strength, tensile cracking strength and E-modulus, as well as the resistance against chloride ions diffusion through the application of high temperature curing treatment [4]. Another advantage is that the final properties are achieved as soon as the high-temperature curing is completed. The drawback is the cost and practical issues if applied at a construction site. Even higher properties can be achieved using high pressure (autoclaving) and temperatures over 150°C [4], but this is not discussed here.

3.   MATERIALS AND EXPERIMENTAL METHODOLOGY

The experimental program aimed at developing and investigating non-proprietary UHPC mixes utilising locally available materials in combination with varying content, types, and a hybrid combination of steel fibres. Two types of aggregate were used in two different UHPC mixes to investigate the influence of variations in the effect of steel fibres in synergy with different aggregates. In the following, a description of the development and production of the local UHPC mixes is given (Section 3.1), along with the experimental program (Section 3.2).

3.1   Development and production of local UHPC

Materials

The materials used for the UHPC mixes consisted of cement, microsilica, fine aggregates, SP, water and two types of steel fibres (micro straight fibres and macro hooked-end fibres). Besides the fine aggregate types and small micro steel fibres, all materials were the same as used in the laboratory to produce conventional concrete. Two aggregate types were applied, both received from suppliers in Norway and being by-products from the production process of crushed gravel. The aggregates were chosen due to their fineness and availability, as well as following the intention of contributing to increasing circular economy through utilisation of by-products. One of the aggregates were filtered harvested dust with D_{max} of 0.6 mm, while the other one was surplus sand with D_{max} of 6 mm. Further information on the constituents is stated in Table 3. The filler aggregate (A1) was pre-treated to ensure a saturated surface dry (SSD) condition, while adjustments in the applied water content during material mixing was applied to account for water adsorption in the crushed sand (A2).

Table 3 – Characteristics of used constituents.

Material	Characteristics	Density [kg/m^3]
Cement (CEM)	CEM I 52.5 N	3100
Microsilica (MS)	Undensified microsilica	2200
Filler sand (A1)	Filter harvest dust from production of gravel (D_{max} = 0.6 mm)	2610
Crushed Sand (A2)	Surplus sand from production of machined gravel (D_{max} = 6 mm)	2770[a]
Superplasticiser (SP)	Modified acrylic polymers, 18% dry content	1060

[a] Obtained from 0-8 mm fraction of the same origin.

The two types of steel fibres, straight micro fibres (SS) and macro hooked-end fibres (HE), are shown in Figure 1 and Table 4 provides some properties given by the manufacturer. The straight micro steel fibres represent the fibre type commonly applied in UHPC, while the macro hooked-end fibre is frequently used in ordinary concrete. The macro hooked-end fibre is introduced due to its lower cost, environmental footprint, and higher availability. Straight micro steel fibres are not used in the traditional concrete industry and had to be imported.
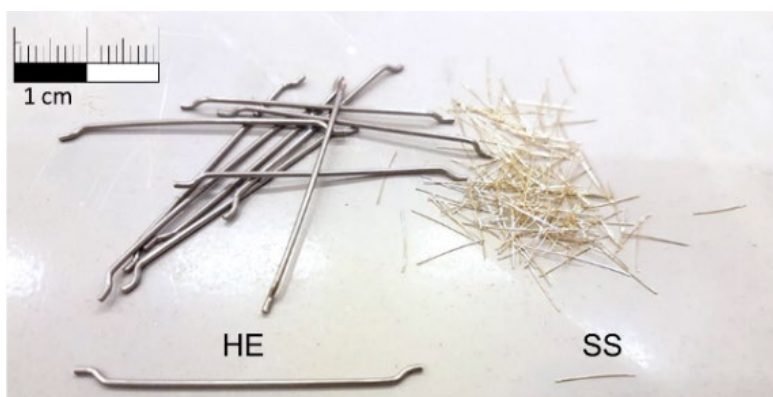

Figure 1 – The two types of steel fibres.

Table 4 – Properties of the steel fibres reported by the manufacturer.

Notation	Shape	l_f [mm]	d_f [mm]	l_f/d_f	Tensile strength [MPa]	E-modulus [GPa]
SS	Straight	13	0.2	65	2600	200
HE	Hooked-end	50	1	50	1100	200

l_f – Fibre length. d_f – Fibre diameter. l_f/d_f – Aspect ratio.

UHPC mix composition

Inspired by the literature review shown in Section 2.1, the following mix proportions were pursued: (i) cement content around 700-800 kg/m³, (ii) microsilica content of 25% of the mass of cement, (iii) a *w/c*-ratio between 0.2 and 0.3, and (iv) an aggregate to cement ratio between 1 and 2. Recommendations on fibre content between 1 and 2 vol.% [6, 29] and D_{max} of 0.8 mm [4] were exceeded in the presented study by including UHPC mixes with lower fibre content and by applying an aggregate type with higher D_{max} in one of the mixes (Mix B).

The particle packing was simulated using the modified Andreasen and Andersen model [33] following (Eq. 1). A q-value of 0.23 was applied, based on recommendations by Yu et al. [28] for materials with high amounts of fines, like UHPC. The software EMMA (Elkem Materials Mix Analyzer) (version 3.5.2) which operates the mathematical model, were used to design the mixes. Both the cumulative PSD curve of the combined dry materials and the target curve is calculated (Eq. 1) in EMMA, and shown in the same diagram, thus illustrating the match of the composed curve towards the target. Figure 2 shows the final PSD of the composed mixes compared to the target curve and the individual PSDs for all dry materials.

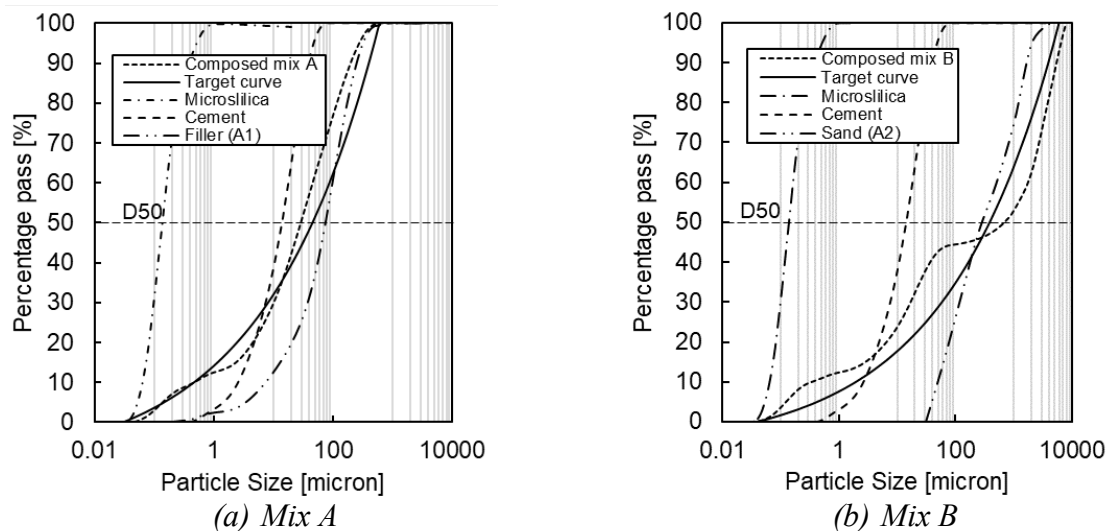| (a) Mix A | (b) Mix B |

Figure 2 – PSDs of the dry constituents, the target curve (modified Andreasen and Andersen curve) and curve of the composed mixes represented in a single-logarithmic plot.

Each constituent was included "as is", without manipulating the fractioning to fit the target curve. Obtaining the best fit to the target curve in EMMA was strived for by adjusting the relative amount of each constituent while maintaining the above-mentioned requirements for mix proportions. The PSDs of the dry materials with D_{max} less than 1 mm were determined through laser diffraction, while sieve analysis was used for larger materials (A2). Assembling measurements from indirect methods like laser diffraction and direct methods like sieving has weaknesses. However, given that no available method, direct or indirect, has the potential for measuring the present span in particle size from 1 nanometre to 10 mm, this procedure has been applied in Figure 2. Table 5 shows the composed UHPC mixes.

Table 5 – Mix composition of the UHPC mixes.

kg/m³												Fresh properties	
Mix	CEM	MS	A1	A2	Wᵃ	SPᵇ	SS	HE	w/c	w/b	vf, %	Airᶜ %	Flowᵈ mm
NF-A	728	182	1237	-	204	13.1	0	-	0.28	0.22	0	5.0	163.7
SS05-A	724	181	1231	-	203	13.0	39	-	0.28	0.22	0.5	4.2	188.7
SS1-A	720	180	1225	-	202	13.0	78	-	0.28	0.22	1	4.2	177.2
SS2-A	713	178	1212	-	200	12.8	156	-	0.28	0.22	2	4.6	192.8
HE2-A	713	178	1212	-	200	12.8	-	156	0.28	0.22	2	3.8	186.3
HY2-A	713	178	1212	-	200	12.8	78	78	0.28	0.22	2	4.0	202.7
SS2-B	756	189	-	1188	170	9.5	156	-	0.22	0.18	2	3.5	142.5
HE2-B	756	189	-	1188	170	9.5	-	156	0.22	0.18	2	3.3	137.5
HY2-B	756	189	-	1188	170	9.5	78	78	0.22	0.18	2	3.5	126.7

CEM – Cement. MS – Microsilica. A1 – Filler sand. A2 – Crushed Sand. W – Water. SP – Superplasticiser. SS – Straight micro steel fibres. HE – Hooked-end fibres. v_f – Volume fraction of steel fibres. ᵃ Including water from SP. ᵇ Solid content. ᶜ EN 12350-7: 2009. ᵈ Final flow, ASTM C230/C230M.

Mixing and specimen fabrication

The UHPCs were mixed at standard laboratory conditions in a laboratory rotating pan-mixer for conventional concrete. The total volume of each batch varied based on the desired number and type of test specimens. The mixing procedure is stated in Table 6 and is similar to the one used by Graybeal [35]. Prior to casting, the rheological properties were measured using a flow table test with a small slump cone (ASTM C230/C230M [36]) often applied for UHPC. The air content was measured according to EN 12350-7:2009 [37]. The average results of the final flow (after jolting the flow table) and air content are shown in Table 5. All specimens were cast in one layer before they were compacted on a vibration table using the procedure given by Graybeal [35], screeded and covered with plastic sheets until demoulding 24 to 48 hours after casting. The casting of the prismatic specimens was done by placing the UHPC in one end of the prism moulds, allowing it to flow to the other end [35].

Table 6 – Mixing procedure.

Process	Time [min]
Mixing of dry materials	10
Adding water and half of the SP while mixing	2
Continue mixing for 1 min before adding the remaining SP over 30 seconds	1.5
Mixing (from powder to thick paste)	10
Adding steel fibres while mixing	2-5
Final mixing	5

Curing at 90°C is an often seen manufacturer-recommended treatment for UHPC [35], which can be challenging to apply in practical construction. In this study three different curing regimes were applied:

1) Submerged in water at 20°C until testing, representing the standard procedure for normal concrete.
2) Moderate heat treatment in water at 45°C for 5 days, then submerged in water at 20°C until testing.
3) Heat treatment in water at 90°C for 48-72 hours (including a gradual increase and decrease of temperature), subsequently submerged in water at 20°C until testing.

3.2   Test program

231 specimens were tested, spanning nine different mixes with two different mix composition and varying steel fibre content, type, and hybrid combination. The two different UHPC mix compositions are denoted Mix A and B in the following. Table 7 gives information about the conducted tests, number and type of test specimen and curing regimes. The flexural test specimens were tested seven to eight days after casting. A Digital Image Correlation (DIC) system was used for observing the behaviour during some of the flexural tests. One series of Mix A was produced to investigate the influence of fibre content by increasing the fibre volume of straight micro steel fibres from 0 to 2%. Another series of Mix A and B was produced to investigate the effects of different fibre types and hybrid combinations when the content was kept constant at 2 vol.%: 100% straight micro fibres (SS), 100% hooked-end fibres (HE) and 50/50 hybrid combination of those (HY).

Table 7 – Test program.

Mix	v_f, %	Mix ID	No. of batches	Tests	Specimens cast	Curing [b]
A	0	NF-A	3	Compressive strength	6 cu, 3 cyl	3
				E-modulus	3 cyl	3
	0.5	SS05-A	3	Compressive strength	6 cu, 3 cyl	3
				E-modulus	3 cyl	3
	1	SS1-A	4	Compressive strength	6 cu, 3 cyl	3
				E-modulus	3 cy	3
	2	SS2-A	4	Compressive strength	36 cu, 12 cyl	1, 3
				Flexural tensile behaviour (DIC)	6 prisms	1
	2	HE2-A	3	Compressive strength	35 cu	1, 3
				Flexural tensile behaviour (DIC)	9 prisms	1
	2	HY2-A	3	Compressive strength	34 cu	1, 3
				Flexural tensile behaviour (DIC)	9 prisms	1
B	2	SS2-B	2	Compressive strength	12 cu	2, 3
				Flexural tensile behaviour	3 prisms	2
	2	HE2-B	2	Compressive strength	12 cu	2, 3
				Flexural tensile behaviour	3 prisms	2
	2	HY2-B	3	Compressive strength	18 cu	2, 3
				Flexural tensile behaviour	6 prisms	2

cu – 100 mm cube. cyl – 100 mm × 200 mm cylinder. prisms – 100 mm × 100 mm × 500 mm prism. [b] 1 – 20°C standard curing. 2 – 45°C moderate heat treatment. 3 – 90°C heat treatment.

Test setups

Figure 3 shows the different test setups. 100 mm cubes were used to measure compressive strength following NS-EN 12390-3:2009 [38]. Cylinders with a diameter of 100 mm and a height of 200 mm were used to measure compressive strength (NS-EN 12390-3:2009 [38]) and E-modulus (NS-EN 12390-13:2013 [39]). The flexural tensile strength was determined using centre-point loading (three-point bending) on prisms of 100 mm × 100 mm × 500 mm at a constant load increment rate of (0.1-0.3 kN/sec). A similar test setup was used in a previous study on the development of local UHPC recipes [12]. The test setup was inspired by ASTM C293 and the flexural strength at peak load was calculated accordingly [40] (Eq. 2):

$$f_t = \frac{3 \cdot P \cdot L}{2 \cdot b \cdot d^2} \tag{2}$$

where P is the peak load, L is the span length, b is the width of the prism, and d is the height. The DIC system was used to monitor the deformation during the flexural tensile tests for the various

fibre combinations of Mix A. The force from the hydraulic machine was matched with the DIC recordings.
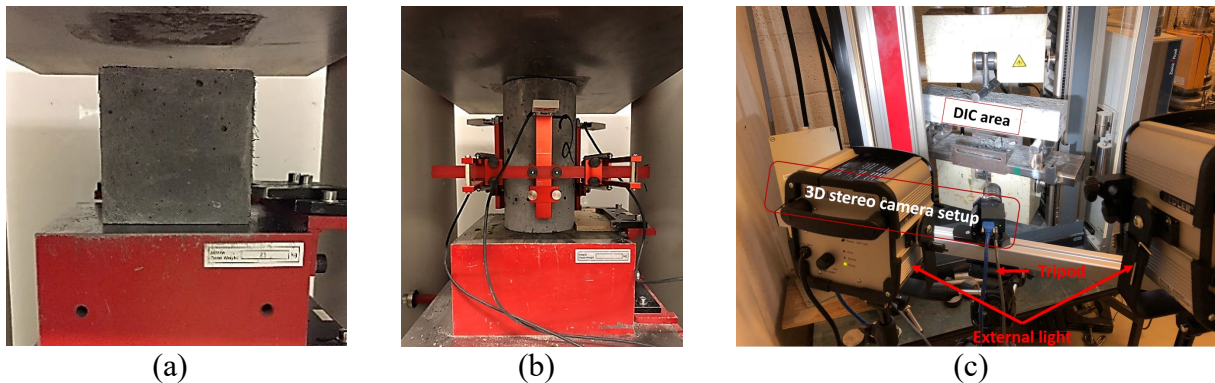

(a) (b) (c)

Figure 3 – Test setups (a) compressive strength, (b) E-modulus and (c) flexural tensile strength with the DIC setup.

Statistical treatment of data
Statistical outliers amongst the results were excluded from the experimental data, before calculating average values. This is implemented as a standard procedure, to secure that the average value from repeated experiments has the best available representativity for the situation. Results were considered to be outliers if it differed more than one and a half time the interquartile range (IQR) below the first quartile (25 percentile, Q1), or above the third quartile (75 percentile, Q3), a procedure described e.g. in [41]. IQR is the difference between Q3 and Q1.

4. EXPERIMENTAL RESULTS AND DISCUSSION

4.1 Strength and behaviour in compression

Influence of content of fibres on compressive strength and E-modulus
Figure 4 (a) shows the average compressive strength and E-modulus of heat-treated UHPC cylinders when varying the content of straight micro steel fibres. All strength results are well above the requirements for UHPC (120 MPa). Both the compressive strength and the E-modulus are minorly influenced by inclusion and variations in fibre content. Similar results have been found in other studies (e.g., in [8, 31]). Yet researchers have found considerable contribution from the fibre reinforcement (e.g., in [23, 24]), making it unclear whether the compressive strength of UHPC is influenced by fibre content. An explanation for positive effects from the fibre reinforcement on compressive strength might be the confining effect of the fibres. However, the addition of fibres might also make the concrete more difficult to cast and in turn give reduced compressive strength. In a recent literature review [26], it is suggested that the seemingly contradictory conclusions might be caused by the shape of the test specimen rather than the actual effects of the fibres. Through the review, it was found that substantial positive influence of the presence of fibres was mainly concluded in investigations using small cubical shaped specimens (40-50 mm), while those using larger cube specimens (100 mm) found some effect, and little influence was found on cylindrical specimens. Figure 4 (b) shows that the cubic samples (cu) in our investigation achieved an increase of 6% for 0.5 vol.% fibres, and about a 10% increase for 2 vol.%, compared to non-fibre reinforced UHPC. No strength increase was observed when using cylindrical specimens. Theoretically, it can be argued that the geometry of test specimens influences stress distribution. The cylindrical shape is often considered to represent the desired

uniaxial stress distribution better than the cubical shape, where the failure is claimed to be more heavily influenced by shear. The results from our investigation strengthen this suggestion, but further investigations with a larger sample size are required to verify this to be the main reason for the contradictions in conclusions on the influence of fibre reinforcement on compressive strength.
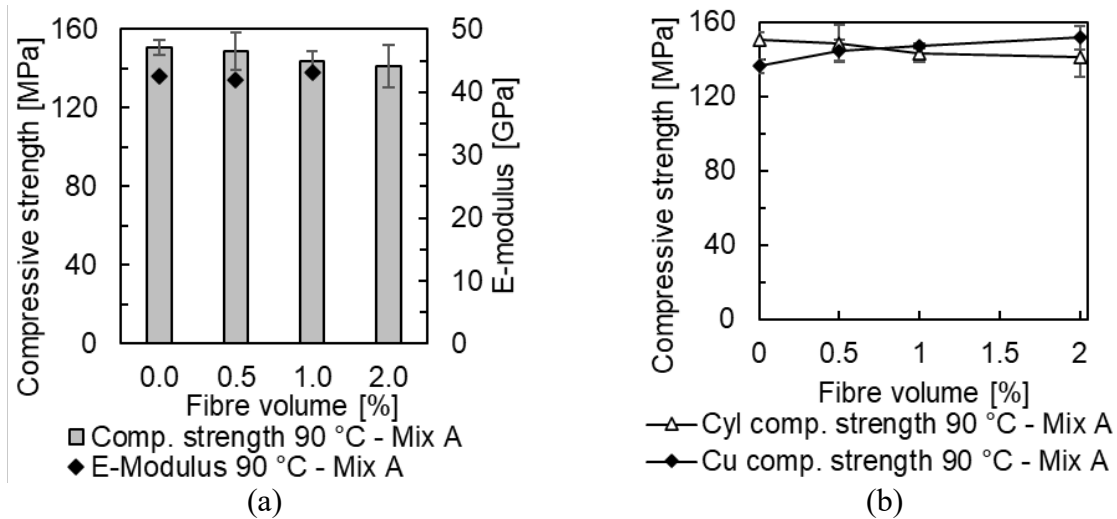

Figure 4 – Average (a) compressive strength and E-modulus of heat-treated cylinders and (b) compressive strength of heat-treated cubes and cylinders. The error bars show the S.D values.

Influence of type and combination of fibres on compressive strength
Figure 5 shows the average cube compressive strength of differently cured specimens with 2 vol.% of either straight steel fibres (SS), hooked-end fibres (HE) or a combination of those two fibres (HY). Little or no impact on the compressive strength was found from variations in fibre type and hybrid combination, whether the curing regime or the UHPC mix composition was altered. Both mixes respond positively to heat curing, as the strength development correlates with curing temperature for all applied levels (20, 45 and 90°C).
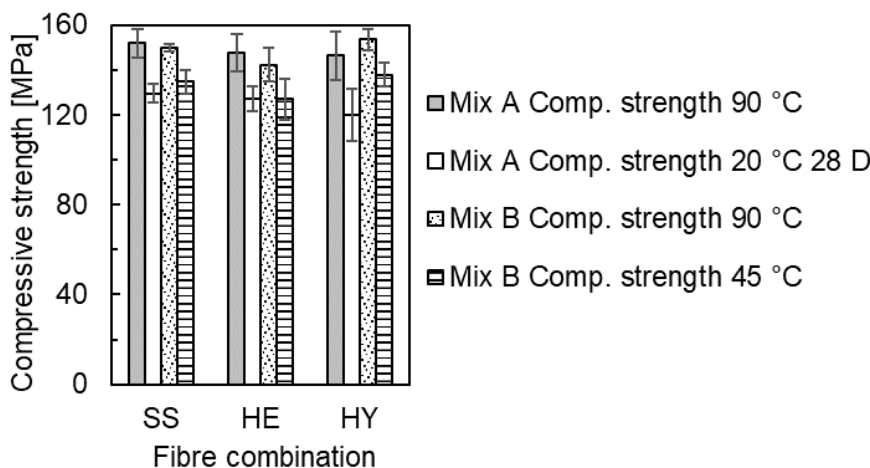

Figure 5 – Average cube compressive strength with 2 vol.% of different fibre types and combination. The error bars show the S.D values.

4.2   Flexural tensile strength and behaviour

Flexural tensile strength
Figure 6 shows the average flexural tensile strength and the corresponding compressive strength at the test day for different types and hybrid combination of steel fibres. The Mix A prisms were exposed to standard curing conditions (20°C), while the Mix B prisms were moderate heat-treated at 45°C. Both test sets were tested seven to eight days after casting. Hence, the Mix B matrix was close to fully matured, while Mix A was still "young". Generally, higher variations in test results can be seen for flexural strength compared to compression and E-modulus results (Figures 4 and 5). This can be explained by the flexural tensile strength being more sensitive than the compressive strength to the presence of fibres, including variations in dispersion and orientation.

Prisms with only macro hooked-end fibres (HE) exhibited the lowest flexural tensile strength. For Mix A prisms, the prisms with straight micro fibres (SS) and hybrid combination (HY) achieved about 60% higher capacity compared to the prisms with only hooked-end fibres. One explanation might be the higher number of fibres in the prisms with straight micro fibres (SS and HY prisms), at constant vol.%. Volume differences of the different fibre types cause the number of straight micro fibres to be 100 times that of hooked-end fibres at fixed vol.%. Hence, the possibility of initiated cracks to be bridged by fibres is much higher for prisms with straight micro fibres. Figure 7 visualises the differences in the number of fibres in cross-sections of the different beam types.

The SS prisms exhibit slightly increased average-strength (5.6%) compared to the HY prisms. From several investigations reported in the literature (e.g., [21, 22, 24]), it is known that hybrid fibre combinations have the potential to increase the tensile properties of UHPC. This is often explained as the synergetic effect from combining fibres with different properties [25], but the effect depends on the applied combination [21, 22].

(a)   (b)
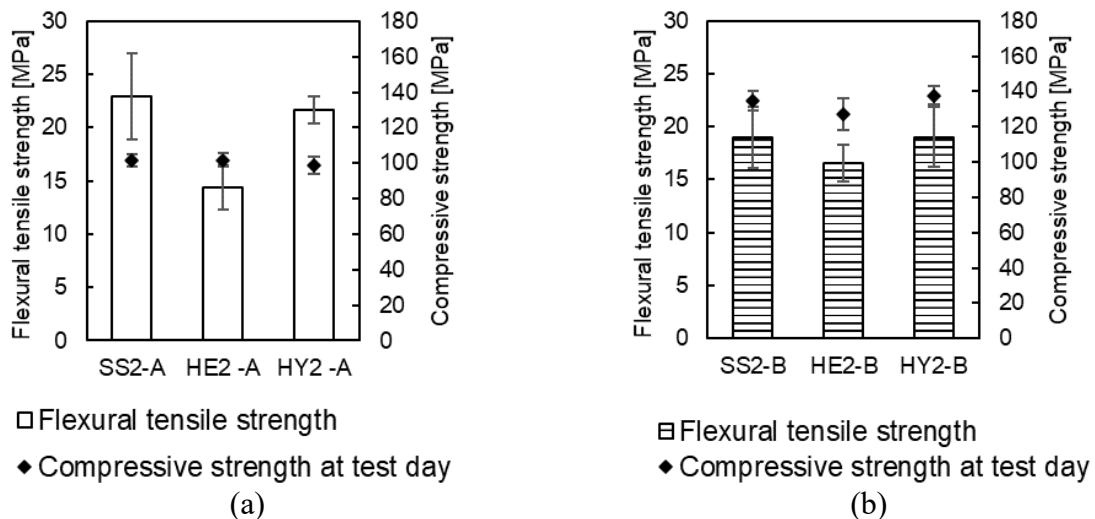
Figure 6 – Average flexural tensile strength of (a) Mix A and (b) Mix B at peak load and cube compressive strength at test day. The error bars show S.D values.

Although hooked-end fibres are generally proven to have considerably higher pull-out capacity than straight fibres [22], this property is not always fully exploitable in UHPC. The explanation is the creation of localised micro-cracks (split cracks) in the cementitious matrix when several fibres with high mechanical anchoring are bundled up in a small volume of matrix [42], also experienced and reported in [21, 30]. This problem where closely located fibres are prone to reduced anchoring is often denoted "fibre group effect" [42]. The risk of this negative effect is greater at high fibre volume fraction, as the fibre bundles is created and consequently matrix

confinement (enveloping) decrease [42]. Figure 7 shows that the HE prisms have several fibre bundles and poor fibre distribution. A better distribution with fewer bundles can be seen for the HY prism with lower content of hooked-end fibres.

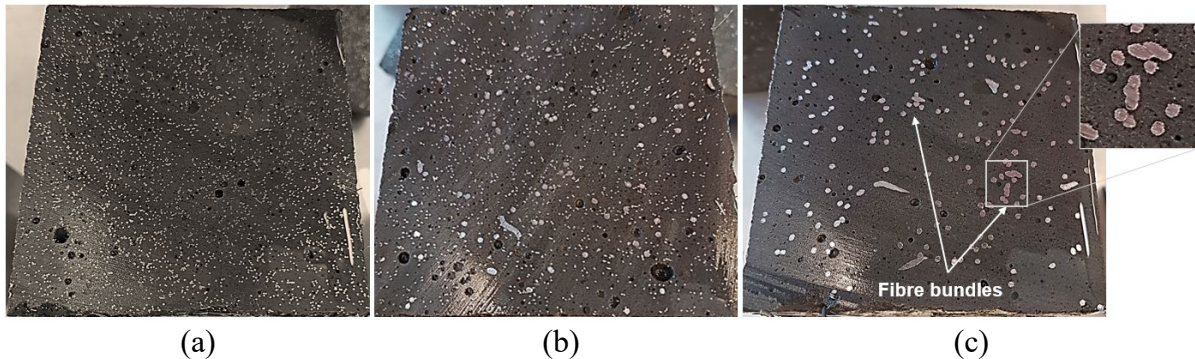| (a) | (b) | (c) |

Figure 7 – Sawn cross-sections with 2 vol.% of (a) straight fibres, (b) hybrid combination of fibres and (c) hooked-end fibres. The cut was made near the critical crack.

The same relative variations in effect between different fibre types were observed for prisms made from Mix B, as for Mix A: SS and HY prisms achieved higher flexural strength than the HE prisms (Figure 6 b). But the positive impact was lower; around 15%. Mix B included a coarser aggregate type than Mix A. Using a coarser aggregate can result in better distribution of macro hooked-end fibres than when introduced to a fine-grained mix [21]. However, the distribution of micro fibres is negatively impacted by the use of coarser aggregate, and also the fibre-matrix bonding of micro fibres have been found weakened [43].

Despite the higher maturity of Mix B than of Mix A at testing day for the prisms (caused by the moderate-heat curing of Mix B), higher capacity was observed for prisms made from Mix A with straight micro fibres (SS and HY prisms). All other variables were kept constant between the two series: the content and types of fibres, specimen geometry and test setup. This supports the idea that the effect of fibre is influenced by other factors than just the fibre type and hybrid combinations. Several differences can be observed that possibly have affected the effectiveness of the fibres. Firstly, the flow values for Mix B were lower than that of Mix A (Table 5). Consequently, it was more difficult to cast, which might have given an adverse effect on the flexural performance by influencing the homogeneity and compactability of the matrix, and the fibre distribution. Secondly, the size of the aggregate differed (Figure 2) which might have caused more defects and pores, poorer distribution of micro fibres and weakened the bonding between the micro fibres and the matrix [43]. Thirdly, the particle packing of the aggregate also differs between the mixes. Figure 2 demonstrates larger deviations between the PSD of the composed Mix B and the target curve than for Mix A. The physical interpretation of these differences is that the particle packing is denser in Mix A than in Mix B. This denser particle packing might affect the bonding between fibres and matrix, emphasising the need for competence and knowledge for utilisation of locally produced UHPC.

The ratio between fibre length and prism cross-section size is known to affect the orientation of fibres, through what is recognised as the wall effect [44]. The wall effect is more profound as the width of the prism tends towards the fibre length [45]. To reduce the influence of the wall effect on the fibre orientation during lab investigations, requirements on the size of the specimen is given in standards for testing normal fibre reinforced concrete (e.g., ASTM C1609 and EN 14651). Due to practical reasons, a cross-section of 100 mm × 100 mm was chosen for this experimental investigation. Thus, the low fibre length to prism cross-section ratio was probably influencing the

orientation of the macro fibres more profoundly than when only using micro fibres. The orientation of fibres is also influenced by other factors, like the flow of the matrix during the casting procedure. Both the fibre length to prism cross-section ratio and the casting process have increased the probability of fibres to orient along the beam axis – yielding higher flexural tensile strength compared to prisms with random fibre orientation. While the influence of the casting procedure concerns both micro and macro fibres, the fibre length to prism cross-section ratio is more influential for the larger hooked-end fibres.

Deformation behaviour

Figure 8 presents the load-displacement curves for selected prisms of Mix A obtained from the DIC system. Three parallel tests for each variable are shown in the figure, along with the average peak load (Av. P_{max}). Mid-point displacement at failure was around 1.5 mm for HE prisms, while for HY and SS prisms the displacement was higher at failure, around 2 to 2.5 mm and 2.5 to 3 mm, respectively. A difference in ductility can be seen in Figure 8 between the beam sets. The prisms with straight micro fibres achieved a more gradual failure. This can be partly explained by a more uniform distribution of fibres and a higher number of fibres crossing the cracks compared to prisms with only hooked-end fibres. Little difference in ductility was observed between the SS and HY prisms. For all beam types, the fibres were pulled out of the matrix and fibre rupture was not observed. Differences in post-peak behaviour could not be registered due to the load-controlled test setup.
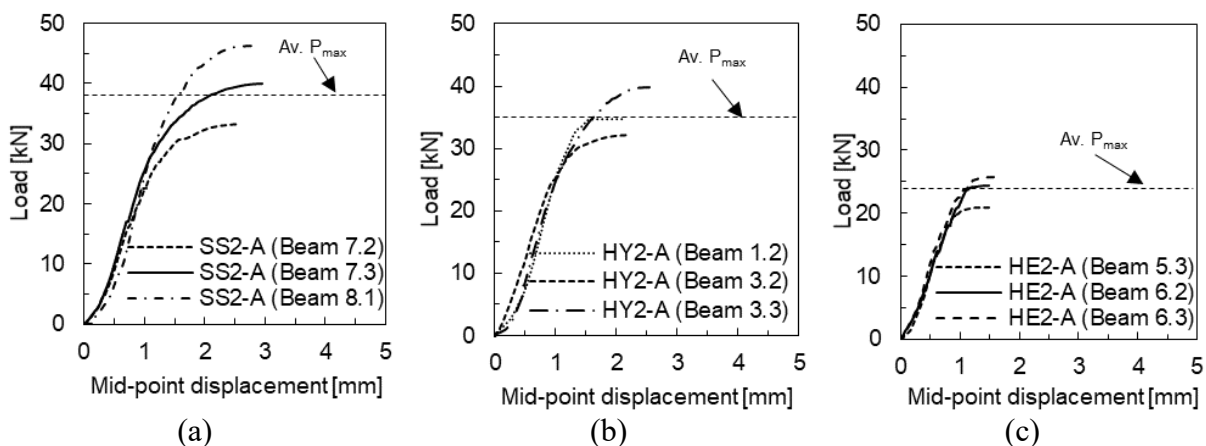

Figure 8 – Load-displacement curves from the DIC measurement for selected UHPC prisms with (a) straight micro fibres (SS), (b) hybrid fibres (HY) and (c) hooked-end fibres (HE). The dotted horizontal line represents the average peak load of the various beam types.

The DIC measurements were used to obtain strain contour plots and crack widths. The cracks were detected by visually identifying high strain gradients from the strain contour plots. Figure 9 shows typical examples of crack patterns at different load stages (15 kN, 20 kN, 30 kN and failure), for the prisms made from Mix A with varying fibre configuration at constant fibre vol.%. The first cracks appeared early in the loading process (first line in Figure 9) in the lower part of the prisms and near the region of the highest bending moment, for all variations of fibre configuration. The prisms including straight micro fibres (SS and HY prisms) developed numerous micro cracks, constantly adding on new cracks as the load increased. For SS prisms, it was not possible to identify at low load levels, which crack would develop into the critical one. However, the prisms with only macro hooked-end fibres (HE prisms) developed a small number of cracks. Later in the loading process, new cracks were only sparsely formed. Rather, the cracks formed at low load levels widened until one crack developed into the critical one. Hence, which crack developing to become the critical one, was observable already at low load levels. The HY

prisms behaved something in between; developing a high number of small cracks, still indicating which crack would develop into the critical one at a lower load level than for the SS prisms.
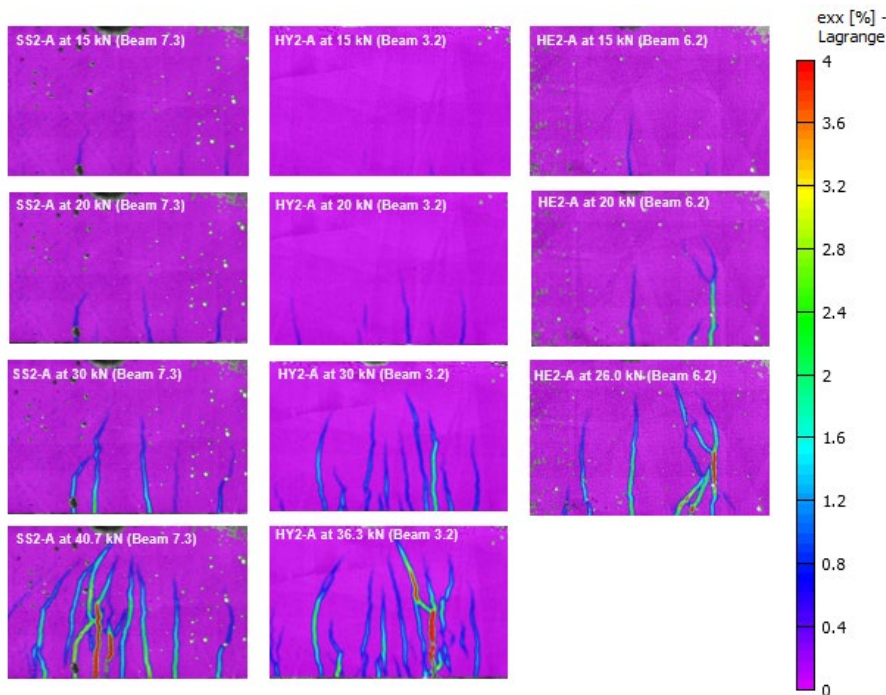

Figure 9 – Selected crack pattern in the area under the load at increasing load levels from DIC strain contour plots (Lagrange strain in the longitudinal direction).

It was possible to track the propagation of the critical crack in each prism by utilising virtual extensometers during the post-processing of the DIC recordings. The result is shown in Figure 10, as a visualisation of propagation of the critical crack for two typical prisms from each beam set.
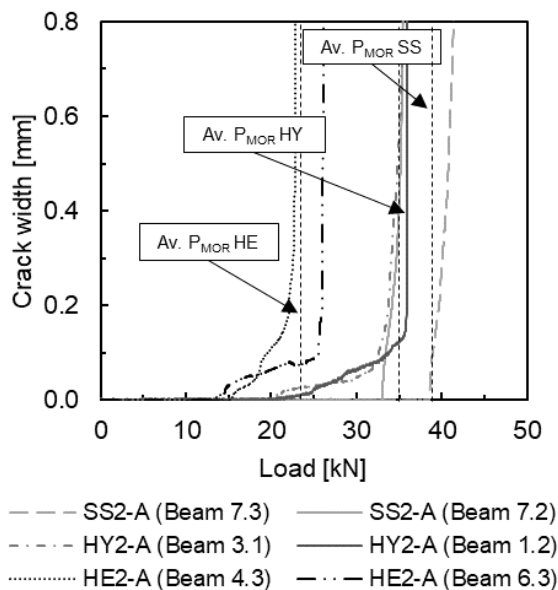

Figure 10 – Selected crack width–load curves of critical cracks. The dotted lines represent the average peak load (Av. P_{MOR}) for each beam type.

The critical crack in the prisms with straight micro fibres (SS) can be seen to form at a later stage of loading than for the other prisms, then propagating steeper. This is consistent with a high number of fibres contributing to a longer multiple cracking phase. The pull-out resistance of each straight micro fibre is low, depending only on the physiochemical bond [46]. When the pull-out of fibres finally occur in what becomes the critical crack, the low remaining capacity allows for the accelerated growth of that crack. Although a steep slope can be observed, the collapse appeared non-brittle (Figure 8). The high number of fibres at the crack surface limited the crack opening at failure. A various number of cracks were formed beside the one that developed to become critical. The average size of these cracks was similar for all beam types and limited to a maximum of 0.3 mm at failure, according to DIC measurements.

The hooked-end fibres have better pull-out properties than the straight micro fibres, due to the longer fibre length and the high mechanical bonding at the end, where the hooks anchor towards the matrix. Thus, the hooked-end fibres bridging the critical crack were capable of delay crack growth and hence having remaining capacity during propagation of the critical crack. This can be seen in Figure 10, as the curve for HE prisms is less steep than for the prisms with only straight micro fibres.

As mentioned in the introduction, there is a risk of rupture of the applied macro fibres. This is due to the relatively low tensile strength (1100 MPa) of these fibres, in combination with a high mechanical anchorage and a high strength matrix. Fibre rupture would have a negative influence on performance and ductility. However, in these experimental investigations (Mix A and B), fibre rupture was not observed. One reason might be the appearance of localised cracks (split cracks) causing premature fibre pullout, as discussed in Section 4.2 *Flexural tensile strength*.

The hooked-end fibres were pulled out of the matrix maintaining the original shape, without straightening of the end-hooks. A visual investigation of the failure zones revealed that cracks appeared near the ends of the fibres (Figure 11). This was also observed by Markovic et al. [47] for dog-bone specimens in direct tension. Straightening of hooked-end fibres leads to an increased pull-out capacity [46], but as the fibre maintained its deformed shape, severe crushing of the surrounding concrete was observed at failure. This fracturing of the matrix phase being the consequence of pull-out of un-deformed hooked-end fibres is visible in the close-up photo in Figure 11. A similar observation of non-straightened hooked-end fibres was also observed and reported in [21, 30].
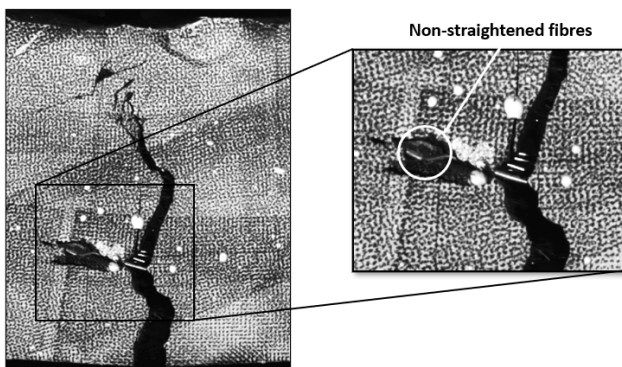

Figure 11 – Non-straightened fibre in one HE prism (Beam 4.1).

The prisms with hybrid fibre combination seemed to benefit from the synergetic effects of the two fibre types. Although the number of fibres was lower for HY prisms than SS prisms, the average

number of cracks at failure was near identical. This might indicate the existence of a critical number of micro fibres, necessary to obtain the multiple-crack development. Unlike SS prisms with the critical crack being identifiable only close to failure load, the critical crack of the HY prisms appeared earlier in the loading process (Figure 10), at a load level around 20 to 25 kN. However, due to the high anchoring properties of the hooked-end fibres, the fibres crossing the critical crack was able to delay further crack propagation. The likelihood of fibre bundling and consequently impaired pull-out capacity for the hooked-end fibres, due to the formation of split cracks, should be reduced compared to the HE prisms, as fewer hooked-end fibres were present in the hybrid fibre combination. This expectation was confirmed by the empirical observation (Figure 7), with fewer fibre bundles observed.

As mentioned above, the synergetic effect of hybrid fibre combination has been found in some investigations to increase the overall performance, compared to single fibre configuration at constant vol.%. The level of gaining from the synergy is, however, depending on specifics in each situation. In our investigations, the synergetic performance of the hybrid fibre combination (HY) was not found to outperform that of single-use of straight micro fibres (SS). However, it was nearly as good. As hooked-end fibres have considerably lower cost and environmental footprint per kg than micro straight steel fibres, this is still a positive effect.

4.3 Comparison to other research and further discussion

Close to 80 UHPC mixes were identified through the papers included in the literature review (Section 2) [12, 20-22, 28, 30, 31]. In addition, four proprietary and commercially available UHPC products were included, with data from [12, 15, 35]. In Figure 12, the average compressive strength of our locally produced UHPC is compared to the strength of both the proprietary and the 80 mixes mentioned above. To compensate for the use of test specimens with different geometry, results using other specimen geometries were converted into equivalent 100 mm cube compressive strength using equations from Wille et al. [9] (Eq. 3 and 4):

$$f_c[\text{cylinder}100 \times 200]/f_c[\text{cube}100] = 0.98 \qquad (3)$$

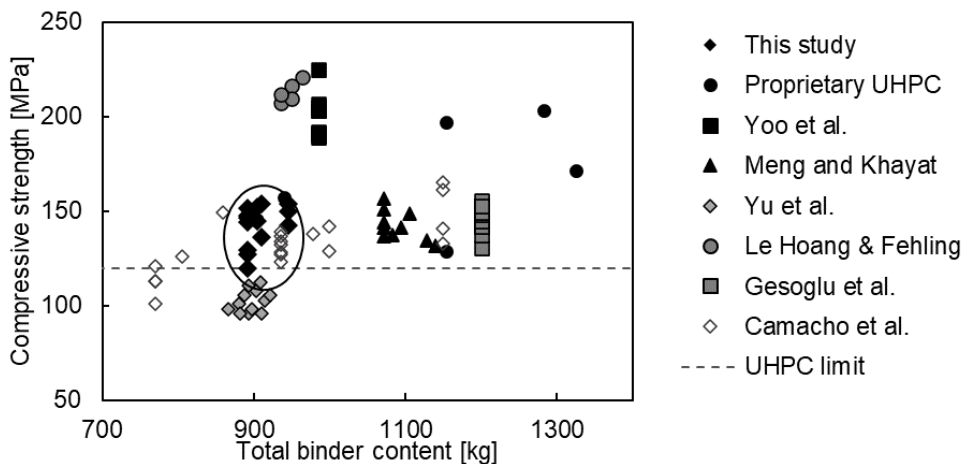$$f_c[\text{cube}50]/f_c[\text{cube}100] = 1.04 \qquad (4)$$

Figure 12 – Comparison between compressive strength (cube 100 mm) in this study (highlighted with a circle) using local materials to proprietary UHPC and UHPC mixes found in research.

Through careful composition, it has been shown easy to prepare UHPC from locally available constituents, performing as good or even better than the proprietary products that are commercially available. Making UHPC with available materials without manipulating PSDs might lead to reduced properties compared to the use of well-composed aggregates or proprietary UHPC products. For industrial purposes, the use of available materials without cost-rising manipulations is often crucial. UHPC class materials might be beneficial for some purposes, even if not fully complying with the UHPC requirements stated in [1] (dotted line in Figure 12). Other qualities than compressive strength might be more important in some applications. One example might be to benefit from the extended durability compared to ordinary concrete, e.g., in the renovation of bridge decks where water tightness is required to delay corrosion of reinforcement in the underlying original structure. Also, UHPC mixes that need curing at elevated temperature to perform better than the requirements stated in [1], might prove to be a better option in terms of cost when utilised without this special curing regime [16].

The flexural strength empirically achieved in this investigation with capacities 18-25 MPa (SS and HY prisms) after only 7 days of curing, was found in line with results found in most of the papers included in Table 2. Higher capacity can be achieved, like those of the proprietary UHPC product presented (Table 2) and the mixes presented by Yoo et al. [21, 30]. Improved flexural capacity could be a result of longer curing or application of heat treatment [4] in line with instructions given by Yoo et al. [21, 30]. However, tensile strength is primarily believed to be influenced by the fibre content. So is the cost and environmental footprint. The price of high strength straight micro fibres is substantially higher than that of ordinary hooked-end macro fibres. Correspondingly is the CO_2 emission, as the micro straight fibres are made from high tensile strength steel through a highly emitting production process (wet wire drawing into small diamters) [18]. Thus, even if the content of micro fibres exceeding 6 vol.% is seen in proprietary UHPC products, it seems wise to adjust the fibre content to meet the requirements for classes of applications. Further benefits might come from investigating potentials indicatively presented in this paper, through partially substituting the straight micro fibres with macro hooked-end fibres, and through optimising the matrix for fibre bonding and distribution.

The opportunity to benefit from adjusting the fibre content to what is strictly needed, from synergies in hybrid fibre configuration and to optimise the matrix for fibre bonding and distribution, seems all to be in favour of UHPC made from locally produced constituents. Correspondingly the potential in using UHPC mixes is made low-cost without manipulating PSDs for optimisation when only certain properties of the UHPC are needed. However, to gain from these opportunities, knowledge and competence on how to produce and manipulate the UHPC is needed.

5.   CONCLUSIONS

The work presented in this paper has shown that it is possible to develop UHPC materials using available constituents by applying simple recommendations on mix proportions and the modified Andreasen and Andersen curve. Compressive strength above 120 MPa was achieved, without applying heat-curing. Even higher compressive strength up to 166 MPa was achieved by applying heat treatment for 48 hours at 90°C. High flexural capacity was demonstrated for prisms, and the deformation behaviour was investigated using a Digital Image Correlation (DIC) camera system. The influence of steel fibre content, type, and hybrid combination in two UHPC mixes can be summarised as follows:

- Neither the compressive strength nor E-modulus of cylinder specimens was found to be influenced by the inclusion or content (vol.%) of steel fibres. A tendency towards a small increase in compressive strength correlating with fibre content was visual for cube specimens. It is suggested that cylindrical specimens simulate the uniaxial conditions better than the cubes and that the appearing strength gains in cubes are attributed to specimen geometry rather than being a material property. The compressive capacity was not found to be affected by variations in fibre type.
- Variations of 60% in flexural strength was found in the fine-grained UHPC mix (Mix A) at a constant level of fibres (2 vol.%) when varying the fibre type from hooked-end macro fibres (HE) to micro fibres (SS). For the coarser mix (Mix B), the corresponding variations were only 15%. Thus, the matrix composition is found to influence the effect of fibres.
- Other factors than just the type and combination of fibres are found to influence the flexural tensile strength of the UHPC, such as flowability, constituent materials and mix design of the matrix. Denser particle packing and smaller aggregate size were found to increase the effect of the straight micro fibres. Consequently, to successfully predict the effect of fibres, also the matrix composition must be considered.
- The hybrid combination (HY) of 50% micro straight steel fibres and 50% hooked-end fibres (2 vol.%) was found to induce similar flexural strength as the exclusive use of straight micro fibres (SS), consistent for both types of UHPC mixes. UHPC with hybrid fibre combination seems to draw synergies by benefiting from the best of each fibre type. Hooked-end fibres are beneficial for reducing CO_2 emissions and cost. Hence, hybrid combinations of fibres demonstrate a potential for gaining the environmental footprint of locally produced UHPC, and to lower the unit price by 30%. There is a risk that especially the macro fibres have an increased tendency to orient along the beam axis due to the wall effect. The consequence would be overestimating the tensile capacity, compared to a situation where the fibres are randomly oriented.
- The opportunity to benefit from four mechanisms seems to be in favour of the development and application of UHPC made from local constituents, compared to the use of proprietary products: i) Adjusting the fibre content to what is strictly needed, ii) synergies from hybrid fibre configuration, iii) optimised matrix composition for fibre bonding and distribution and iv) producing low-cost UHPC mixes without manipulating PSDs for optimisation, when only certain properties of the UHPC are needed. However, to gain from these opportunities, knowledge and competence on how to produce and manipulate the UHPC is needed.

ACKNOWLEDGEMENTS

REFERENCES

1. Graybeal B, Brühwiler E, Kim B-S, Toutlemonde F, Voo Y L & Zaghi A: "International Perspective on UHPC in Bridge Engineering". *Journal of Bridge Engineering,* Vol. 25, No. 11, 2020, p. 04020094.
2. Naaman A E & Wille K: "The path to ultra-high performance fiber reinforced concrete (UHP-FRC): five decades of progress". *Proceedings*, HiPerMat 2012, 3rd International Symposium on UHPC and Nanotechnology for High Performance Construction Materials, Kassel, Germany, March 2012, pp. 3-15.
3. Azmee N M & Shafiq N: "Ultra-high performance concrete: From fundamental to applications". *Case Studies in Construction Materials,* Vol. 9, 2018, p. e00197.
4. Russell H G & Graybeal B A: "Ultra-high performance concrete: A state-of-the-art report for the bridge community". FHWA Publication No.: FHWA-HRT-13-060, Federal Highway Administration, United States, 2013, p. 171.
5. Alkaysi M & El-Tawil S: "Effects of variations in the mix constituents of ultra high performance concrete (UHPC) on cost and performance". *Materials and Structures,* Vol. 49, No. 10, 2016, pp. 4185-4200.
6. Graybeal B A: "Development of Non-Proprietary Ultra-High Performance Concrete for Use in the Highway Bridge Sector". FHWA Publication No.: FHWA-HRT-13-100, Federal Highway Administration, United States, 2013, p. 8.
7. Larsen I L, Terjesen O, Thorstensen R T & Kanstad T: "Use of Concrete for Road Infrastructure: A SWOT Analysis Related to the three Catchwords Sustainability, Industrialisation and Digitalisation". *Nordic Concrete Research,* Vol. 60, No. 1, 2019, p. 31.
8. Alsalman A, Dang C N & Hale W M: "Development of ultra-high performance concrete with locally available materials". *Construction and Building Materials,* Vol. 133, 2017, pp. 135-145.
9. Wille K, Naaman A E & Parra-Montesinos G J: "Ultra-High Performance Concrete with Compressive Strength Exceeding 150 MPa (22 ksi): A Simpler Way". *ACI Materials Journal,* Vol. 108, No. 1, 2011, pp. 46-54.
10. Fidjestol P, Thorsteinsen R & Svennevig P: "Making UHPC with local materials—the way forward". *Proceedings*, HiPerMat 2012, 3rd International Symposium on UHPC and Nanotechnology for High Performance Construction Materials, Kassel, Germany, March 2012, pp. 207-214.
11. Jacobsen S, Haugen L C & Arntsen B: "Developing Ultra High Performance Concrete for concrete products". *Nordic Concrete Research,* Vol. 33, No. 1, 2005, pp. 156-158.
12. Camacho E, López J Á & Serna P: "Definition of three levels of performance for UHPFRC-VHPFRC with available materials". *Proceedings*, HiPerMat 2012, 3rd international symposium on UHPC and Nanotechnology for high performance construction materials, Kassel, 2012, pp. 249-256.
13. Bache H H: "Introduction to compact reinforced composite". *Nordic Concrete Research,* Vol. 6, 1987, pp. 19-33.
14. Martius-Hammer T A, Wagner E, Schramm R, Fosså K T & Berge J: "Construction of large UHPC structures - Experience from a slipforming mock-up test". *Proceedings*, FIB 2018 - Proceedings for the 2018 fib Congress: Better, Smarter, Stronger, 2019, pp. 3571-3580.
15. Aarup B, Jensen L R & Ellegaard P: "Slender CRC columns". *Nordic Concrete Research,* Vol. 34, No. 2, 2005, pp. 80-97.
16. Aarup B K: "A type of UHPC not quite up to standards". *Proceedings*, AFGC-ACI-fib-RILEM Int. Symposium on Ultra-High Performance Fibre-Reinforced Concrete (UHPFRC 2017), Montpellier, France, October 2017, Vol. 2, pp. 965-974.

17. Bergsagel D, Granlund M, Klausen S S & Skårnes A: "Ultra-high performance concrete (UHPC) – The influence of curing regime, fibre and aggregate". ("Ultrahøyfast betong (UHPC) – Innvirkning av herderegime, fiber og sand på betongens egenskaper"). Bachelor Thesis, University of Agder, Department of Engineering Sciences, Grimstad, Norway, 2020. (in Norwegian).

18. Stengel T & Schießl P: "Sustainable construction with UHPC–from life cycle inventory data collection to environmental impact assessment". *Proceedings*, Second International Symposium on Ultra High Performance Concrete, Kassel, Germany, March 2008, pp. 461-468.

19. Yoo D Y, Kang S T & Yoon Y S: "Enhancing the flexural performance of ultra-high-performance concrete using long steel fibers". *Composite Structures,* Vol. 147, 2016, pp. 220-230.

20. Gesoglu M, Güneyisi E, Muhyaddin G F & Asaad D S: "Strain hardening ultra-high performance fiber reinforced cementitious composites: Effect of fiber type and concentration". *Composites Part B: Engineering,* Vol. 103, 2016, pp. 74-83.

21. Yoo D Y, Kim M J, Kim S W & Park J J: "Development of cost effective ultra-high-performance fiber-reinforced concrete using single and hybrid steel fibers". *Construction and Building Materials,* Vol. 150, 2017, pp. 383-394.

22. Meng W & Khayat K H: "Effect of Hybrid Fibers on Fresh Properties, Mechanical Properties, and Autogenous Shrinkage of Cost-Effective UHPC". *Journal of Materials in Civil Engineering,* Vol. 30, No. 4, 2018, p. 04018030.

23. Wu Z, Shi C, He W & Wu L: "Effects of steel fiber content and shape on mechanical properties of ultra high performance concrete". *Construction and Building Materials,* Vol. 103, 2016, pp. 8-14.

24. Wu Z, Shi C, He W & Wang D: "Static and dynamic compressive properties of ultra-high performance concrete (UHPC) with hybrid steel fiber reinforcements". *Cement and Concrete Composites,* Vol. 79, 2017, pp. 148-157.

25. Markovic I: "High-performance hybrid-fibre concrete: development and utilisation". PhD Thesis, Delft University of Technology, Civil Engineering and Geosciences, Delft, The Netherlands, 2006, 228.

26. Larsen I L & Thorstensen R T: "The influence of steel fibres on compressive and tensile strength of ultra high performance concrete: A review". *Construction and Building Materials,* Vol. 256, 2020, p. 119459.

27. Richard P & Cheyrezy M: "Composition of reactive powder concretes". *Cement and Concrete Research,* Vol. 25, No. 7, 1995, pp. 1501-1511.

28. Yu R, Spiesz P & Brouwers H J H: "Development of an eco-friendly Ultra-High Performance Concrete (UHPC) with efficient cement and mineral admixtures uses". *Cement and Concrete Composites,* Vol. 55, 2015, pp. 383-394.

29. Wille K & Boisvert-Cotulio C: "Material efficiency in the design of ultra-high performance concrete". *Construction and Building Materials,* Vol. 86, 2015, pp. 33-43.

30. Yoo D Y, Kim S, Park G J, Park J J & Kim S W: "Effects of fiber shape, aspect ratio, and volume fraction on flexural behavior of ultra-high-performance fiber-reinforced cement composites". *Composite Structures,* Vol. 174, 2017, pp. 375-388.

31. Le Hoang A & Fehling E: "Influence of steel fiber content and aspect ratio on the uniaxial tensile and compressive behavior of ultra high performance concrete". *Construction and Building Materials,* Vol. 153, 2017, pp. 790-806.

32. Shi C, Wu Z, Xiao J, Wang D, Huang Z & Fang Z: "A review on ultra high performance concrete: Part I. Raw materials and mixture design". *Construction and Building Materials,* Vol. 101, 2015, pp. 741-751.

33. Funk J E & Dinger D R: "Derivation of the Dinger-Funk Particle Size Distribution Equation". "Predictive Process Control of Crowded Particulate Suspensions: Applied to Ceramic Manufacturing", Springer US, Boston, MA, 1994, pp. 75-83.

34. Andreasen A H M & Andersen J: "On the relationship between grain gradation and space in products made from loose grains (with some experiments)". ("Ueber die Beziehung zwischen Kornabstufung und Zwischenraum in Produkten aus losen Körnern (mit einigen Experimenten"). *Kolloid-Zeitschrift,* Vol. 50, No. 3, 1930, pp. 217-228. (in German)

35. Graybeal B A: "Material property characterization of ultra-high performance concrete". FHWA Publication No.: FHWA-HRT-06-103, Federal Highway Administration, United States, 2006, p. 186.

36. ASTM International: "ASTM C230/C230M-14 , Standard Specification for Flow Table for Use in Tests of Hydraulic Cement". West Conshohocken, PA, United States, 2014, p. 7.

37. European Committee for Standardization: "NS-EN 12350-7: 2009, Testing fresh concrete: Air content–Pressure methods". NS-EN 12350-7: 2009, Brussels, Belgium, 2009, p. 28.

38. European Committee for Standardization: "NS-EN 12390-3:2009, Testing hardened concrete - Part 3: Compressive strength of test specimens". NS-EN 12390-3:2009, Brussels, Belgium, 2009, p. 24.

39. European Committee for Standardization: "NS-EN 12390-13:2013, Testing hardened concrete - Part 13: Determination of secant modulus of elasticity in compression". NS-EN 12390-13:2013, Brussels, Belgium, 2014, p. 20.

40. ASTM International: "ASTM C293 / C293M-16, Standard Test Method for Flexural Strength of Concrete (Using Simple Beam With Center-Point Loading)". West Conshohocken, PA, United States, 2016, p. 4.

41. Del Monte E, Boschi S & Vignoli A: "Prediction of compression strength of ancient mortars through in situ drilling resistance technique". *Construction and Building Materials,* Vol. 237, 2020, p. 117563.

42. Wille K, Xu M, El-Tawil S & Naaman A E: "Dynamic impact factors of strain hardening UHP-FRC under direct tensile loading at low strain rates". *Materials and Structures/Materiaux et Constructions,* Vol. 49, No. 4, 2016, pp. 1351-1365.

43. Xu L, Wu F, Chi Y, Cheng P, Zeng Y & Chen Q: "Effects of coarse aggregate and steel fibre contents on mechanical properties of high performance concrete". *Construction and Building Materials,* Vol. 206, 2019, pp. 97-110.

44. Raju R A, Lim S, Akiyama M & Kageyama T: "Effects of concrete flow on the distribution and orientation of fibers and flexural behavior of steel fiber-reinforced self-compacting concrete beams". *Construction and Building Materials,* Vol. 262, 2020, p. 119963.

45. Boulekbache B, Hamrat M, Chemrouk M & Amziane S: "Flowability of fibre-reinforced concrete and its effect on the mechanical properties of the material". *Construction and Building Materials,* Vol. 24, No. 9, 2010, pp. 1664-1671.

46. Abdallah S, Fan M & Rees D W: "Bonding mechanisms and strength of steel fiber–reinforced cementitious composites: overview". *Journal of Materials in Civil Engineering,* Vol. 30, No. 3, 2018, p. 04018001.

47. Markovic I, Walraven J & Van Mier J: "Tensile behaviour of high performance hybrid fibre concrete". *Proceedings*, 5th International Symposium on Fracture Mechanics of Concrete and Concrete Structures, Vail Colorado, 2004, Vol. 2, pp. 1113-1121.